Relativistic solitary waves with phase modulation embedded in long laser pulses in plasmas

G. Sanchez-Arriaga, E. Siminos and E. Lefebvre

CEA, DAM, DIF, 91297 Arpajon, France

Abstract

We investigate the existence of nonlinear phase-modulated relativistic solitary waves embedded in an infinitely long circularly polarized electromagnetic wave propagating through a plasma. These states are exact nonlinear solutions of the 1-dimensional Maxwell-fluid model for a cold plasma composed of electrons and ions. The solitary wave, which consists of an electromagnetic wave trapped in a self-generated Langmuir wave, presents a phase modulation when the group velocity V and the phase velocity V_{ph} of the long circularly polarized electromagnetic wave do not match the condition $VV_{ph} = c^2$. The main properties of the waves as a function of their group velocities, wavevectors and frequencies are studied, as well as bifurcations of the dynamical system that describes the waves when the parameter controlling the phase modulation changes from zero to a finite value. Such a transition is illustrated in the limit of small amplitude waves where an analytical solution for a grey solitary wave exists. The solutions are interpreted as the stationary state after the collision of a long laser pulse with an isolated solitary wave.

I. INTRODUCTION

The progress in laser technology has provided the conditions to investigate previously unattainable regimes in laser-plasma interaction and also to test physical theories such as the dynamics of nonlinear waves in plasmas. A topic that has received great attention is the existence of solitary waves produced during the interaction of a high-intensity laser pulse with an underdense plasma. These waves are excited by the downshifting of a fraction of the incident laser pulse that, when it reaches a frequency below the local Langmuir frequency, becomes trapped inside a related electron density cavity [1, 2]. In this cavity, the electrostatic force due to charge separation is balanced by the ponderomotive force of the trapped wave. The theoretical works, most of them carried out in the framework of the fluid plasma model (see Ref. 3 for a summary), together with the solitary waves observed in one [4], two [1, 2, 5, 6] and three [7–9] dimensional particle-in-cell simulations have laid the foundations of our current understanding of these electromagnetic structures. Such knowledge is now crucial to interpret the recent laboratory experiments where solitary waves (or their signatures) have been observed [9–15].

Even though the warm [16, 17] and magnetized [18, 19] plasmas have been also considered, the properties of the solitary waves have been mainly investigated within the cold, relativistic, one-dimensional fluid approximation [3, 17–30]. This theory assumes a circularly polarized vector potential with components normal to the direction of propagation x given by

$$A_y + iA_z = a(\xi) exp\left\{i\left[kx - \omega t + \theta(\xi)\right]\right\} \tag{1}$$

where ξ is the coordinate in a frame moving with the group velocity V, ω is the frequency and k the wavevector. Taking only variations with ξ, substituting this vector potential in the Maxwell-fluid equations and imposing either vanishing (VBC) or nonvanishing (NVBC) boundary conditions at $\xi \to -\infty$, the partial differential equations become three ordinary differential equations for the amplitude a, the potential ϕ and the phase θ. The variables a and ϕ are governed by two second order differential equations that describe Langmuir and electromagnetic waves coupled by the nonlinear term arising from the perturbation of the density and relativistic mass. The variable θ is decoupled and can be calculated once a and ϕ are known. Even though the system is not completely integrable the solitary waves solutions are commonly referred to as solitons.

The set of ordinary differential equations for a and ϕ has a Hamiltonian structure and certain symmetries (i.e. it is ξ-reversible), and can be investigated by directly applying the theory of dynamical systems. However, it is important to note that not all solutions of this Hamiltonian system are physically relevant; only solutions connecting a certain fixed point in phase space are consistent with the boundary conditions imposed to the original partial differential equations at $\xi \to -\infty$. We also recall that solitary waves are homoclinic or heteroclinic orbits to such a fixed point and they lie in the intersection of its stable and unstable manifolds. Therefore the existence and stability properties of the fixed point play a central role, as they determine the domains in the $V-\omega-k$ parametric space where solitary waves may exist (as well as the properties of the spectrum of solutions). For instance, in parametric domains where the fixed point is a center, a saddle-center or a saddle-focus, one expects to have no solutions, branches of solutions or a continuum, respectively (except for very particular cases, i.e. resonances [31]). This result can be inferred by taking into account the dimension of phase space and the dimension of the stable and unstable manifolds of the fixed point. Unless further restrictions exist, the continuous spectrum detected in domains where the fixed point is a saddle-center [3, 28, 29] may be considered a numerical artefact.

For VBC, $a \to 0$ and $\phi \to 0$ as $\xi \to -\infty$, the solitary waves are commonly named bright solitons and they represent a light wave trapped in a self-generated plasma wave [24]. They are homoclinic orbits to the fixed point of the Hamiltonian system and therefore $a \to 0$ and $\phi \to 0$ as $\xi \to +\infty$. In this case the Maxwell-fluid model only admits solutions if the phase velocity $V_{ph} \equiv \omega/k$ and the group velocity V satisfy the relation $VV_{ph} = c^2$ and the phase θ is constant. The problem has two free parameters, the fixed point where the orbit connects is a saddle-center, and the solutions are organized in the $V-\omega$ plane in branches where the vector potential has different numbers of zeros or humps [27]. The branches end at a critical velocity where the ions density profile shows a cusp. This soliton breaking has been proposed as a mechanism of ion acceleration [27]. For fixed ions and V=0, an analytical solution can be found and solitary waves exist within a continuous range of ω [26].

In the case of nonvanishing boundary conditions (NVBC), $a \to a_0$ and $\phi = 0$ as $\xi \to -\infty$, the solutions of the system represent a solitary electromagnetic wave trapped in a self-generated Langmuir wave and embedded in an infinitely long circularly polarized electromagnetic wave. Crudely speaking, a solitary wave with NVBC can be considered as a wave with VBC but embedded in a long laser pulse with amplitude a_0. For this case the system

does not require any condition relating V, ω and k and in general there is also a modulation in the phase. The amplitude a_0 is linked to ω and k by the dispersion relationship of a circularly polarized electromagnetic wave in a plasma, a relation that naturally appears in the dynamical system as the condition of existence of the fixed point where the solitary wave connects. Previous works have investigated these waves in the particular case $VV_{ph} = c^2$ [3, 29, 30]. Under this assumption, there are only two free parameters, for instance V and ω, and the solutions have no phase modulation. Depending on the behaviour of the solitary waves at $\xi \to +\infty$, it is possible to construct three different kinds of solutions: (i) grey solitons ($a \to a_0$ and $\phi \to 0$), (ii) dark solitons ($a \to -a_0$ and $\phi \to 0$) and (iii) shock waves ($a \to 0$ and $\phi \to \phi_0$). Note that the grey solitons are homoclinic orbits whereas the dark solitons and the shock waves are heteroclinic orbits. The solitary waves are organized in branches in parameter regions where the fixed point is a saddle-center [3, 29] and in a continuum if it is a saddle-focus [30].

Here we consider solitary waves with NVBC and, as opposed to previous works, we do not assume the restriction $VV_{ph} = c^2$. The relaxation of this condition has three effects: (i) the solitary waves present a nonlinear phase modulation, (ii) there is an additional parameter in the analysis and (iii) the topology of the phase space is drastically changed due to the appearance of a new term in the equations that diverges as $a \to 0$. The organization of the paper is as follows. In Sec. II the equations that govern the dynamics of the solitary wave are derived from the Maxwell-fluid model. In Sec. III the small amplitude limit is explored and an analytical solution for a grey solitary wave found. This solution illustrates some features of the dynamics that are present for arbitrary large amplitudes. The arbitrary large amplitude case is considered in Sec. IV, where we study the stability properties of the fixed point and we present some numerically computed solutions. The conclusions are summarized in Sec. V. Finally, the appendix A shows that solitary waves with modulated phase do not exist in the limit of $V = 0$ with immobile ions.

II. THE FLUID MODEL

The solitary waves are studied in the framework of the Maxwell-fluid model. The plasma is assumed to be cold and composed of electrons and ions that are denoted by the subscript $\alpha = e, i$ respectively. For convenience, we normalize the length, time, velocity, momentum,

vector and scalar potential, and density to c/ω_{pe}, ω_{pe}^{-1}, c, $m_\alpha c$, $m_e c^2/e$ and n_0 respectively. Here n_0, m_α and $\omega_{pe}^2 = 4\pi n_0 e^2/m_e$ are the unperturbed density, rest mass and electron plasma frequency, respectively. Using this notation Maxwell's (in the Coulomb gauge) and plasma equations are

$$\Delta\phi = n_e - n_i \tag{2a}$$

$$\Delta\mathbf{A} - \frac{\partial^2\mathbf{A}}{\partial t^2} - \frac{\partial}{\partial t}\nabla\phi = n_e\mathbf{v}_e - n_i\mathbf{v}_i \tag{2b}$$

$$\frac{\partial n_\alpha}{\partial t} + \nabla\cdot(n_\alpha\mathbf{v}_\alpha) = 0 \tag{2c}$$

$$\frac{\partial\mathbf{P}_\alpha}{\partial t} - \mathbf{v}_\alpha\times(\nabla\times\mathbf{P}_\alpha) = -\nabla\left(\epsilon_\alpha\phi + \gamma_\alpha\right) \tag{2d}$$

where $\mathbf{A}$ and ϕ are the vector and scalar potentials, $\mathbf{P}_\alpha \equiv \mathbf{p}_\alpha + \epsilon_\alpha\mathbf{A}$, $\gamma_\alpha \equiv (1+|\mathbf{p}_\alpha|^2)^{1/2}$ and $\mathbf{p}_\alpha$ and $\mathbf{v}_\alpha \equiv \mathbf{p}_\alpha/\gamma_\alpha$ are the kinetic momentum and the fluid velocity respectively. For convenience the dimensionless parameter $\epsilon_\alpha \equiv (q_\alpha m_e)/(e m_\alpha)$ has been introduced ($q_e = -e$ and $q_i = e$ are the charges of the species).

Assuming $\partial_y = \partial_z = 0$, the Coulomb gauge gives $\mathbf{A} = \mathbf{A}_\perp$ and Eq. (2d) yields $\mathbf{P}_{\perp\alpha} = 0$. Here $\perp$ denotes the direction perpendicular to x. For convenience we will take a definition for the vector potential and the variable ξ slightly different from the one introduced in Sec. I. In particular, we take all variables to be functions of $\xi = (x - Vt)/\sqrt{1-V^2}$, and write the normalized circularly polarized vector potential as

$$A_y + iA_z = a(\xi) exp\left[\frac{i\left(kx-\omega t\right)}{\sqrt{1-V^2}} + i\theta(\xi)\right] \tag{3}$$

where ω and k are the frequency and the wavevector in a frame moving with the group velocity of the solitary wave V. By imposing the boundary condition $a = a_0$, $\phi = 0$, $n_\alpha = 1$ and $p_{x\alpha} = 0$ as $\xi \to -\infty$, the longitudinal component of Eq. (2d), Eq. (2c) and the definition of the γ_α factors yield $n_\alpha(\phi, a) = V\left(\psi_\alpha/r_\alpha - V\right)/(1-V^2)$, $\gamma_\alpha = (\psi_\alpha - V r_\alpha)/(1-V^2)$ and $v_\alpha = (V\psi_\alpha - r_\alpha)/(\psi_\alpha - V r_\alpha)$ where we introduced the following auxiliary variables $\psi_\alpha(a,\phi) \equiv \Gamma_\alpha - \epsilon_\alpha\phi$, $r_\alpha(a,\phi) \equiv \left[\psi_\alpha^2 - (1-V^2)(1+\epsilon_\alpha^2 a^2)\right]^{1/2}$ and $\Gamma_\alpha = (1+\epsilon_\alpha^2 a_0^2)^{1/2}$. Substituting these results in Eqs. (2a) and (2b) yields [3, 29]

$$a'' = \left[V\left(\frac{1}{r_e} + \frac{\epsilon}{r_i}\right) - \left(\bar{\omega}^2 - \bar{k}^2\frac{a_0^4}{a^4}\right)\right]a \tag{4}$$

$$\phi'' = V\left(\frac{\psi_e}{r_e} - \frac{\psi_i}{r_i}\right) \tag{5}$$

$$\theta' = -\bar{k}\left(1 - \frac{a_0^2}{a^2}\right) \tag{6}$$

where $\bar{k} \equiv (k - V\omega)/(1 - V^2)$ and $\bar{\omega} \equiv (\omega - Vk)/(1 - V^2)$ and for brevity we also wrote $\epsilon_i \to \epsilon$.

Equations (4) and (5) describe the dynamics of localized electromagnetic modulations trapped by a self-generated Langmuir wave embedded in an infinitely long circularly polarized electromagnetic wave. Both equations are decoupled from Eq. (6) that describes the modulation in the phase. Note that, as $\xi \to -\infty$, one has $a \to a_0$ and the solution becomes a circularly polarized electromagnetic wave with phase velocity $V_{ph} = \omega/k$. We see that the solutions have no phase modulation if the phase velocity and the group velocity satisfy the condition $VV_{ph} = 1$ or if there is no solitary wave $[a(\xi) = a_0]$.

System (4-5) is a ξ-reversible fourth order Hamiltonian system with Hamiltonian

$$H(a, P_a, \phi, P_\phi) = \frac{1 - V^2}{2}\left[\left(\frac{P_a}{1 - V^2}\right)^2 + \bar{\omega}^2 a^2 + \bar{k}^2 \frac{a_0^4}{a^2}\right] + V\left[r_e(a, \phi) + \frac{r_i(a, \phi)}{\epsilon}\right] - \frac{1}{2}P_\phi^2 \qquad (7)$$

where the momenta are given by $P_a = (1 - V^2)a'$ and $P_\phi = -\phi'$. The Hamiltonian is constant since it does not depend on ξ. Another interesting property is the existence of the fixed points $Q_0^\pm$ defined by $(\phi, \phi', a, a') = (0, 0, \pm a_0, 0)$ if the following relation is satisfied

$$\bar{\omega}^2 = \bar{k}^2 + \frac{1}{\Gamma_e} + \frac{\epsilon}{\Gamma_i} \qquad (8)$$

The physical interpretation of this condition is evident if we rewrite it as [32]

$$\omega_{LF}^2 = k_{LF}^2 + \frac{1}{\Gamma_e} + \frac{\epsilon}{\Gamma_i} \qquad (9)$$

where $\omega_{LF} \equiv \omega/\sqrt{1 - V^2}$ and $k_{LF} \equiv k/\sqrt{1 - V^2}$ are the frequency and the wavevector in the laboratory frame. Therefore, Eq. (8) is the dispersion relation of a pure transverse circularly polarized electromagnetic wave with relativistic amplitude and mobile ion effects. It has a solution within the frequency range $\bar{k} \equiv \bar{\omega}_{min} < \bar{\omega} < \bar{\omega}_{max} \equiv \sqrt{1 + \epsilon + \bar{k}^2}$.

In order to be consistent with the boundary conditions imposed to the original partial differential equations [Sys. (2)], the solitary waves must connect with the fixed point Q_0^+ as $\xi \to -\infty$. In the particular case $\bar{k} = 0$ there is another fixed point Q_1 given by $(\phi, \phi', a, a') = [(\Gamma_i - \Gamma_e)/(1 + \epsilon), 0, 0, 0]$. An orbit connecting Q_0^+ with Q_1 is referred to as a shock wave [3, 29] and it exists for velocity values [30]

$$V_S = \frac{\epsilon a_0^2}{2\Gamma_e\Gamma_i}\left[\left(1 - \frac{\epsilon a_0^2}{2\Gamma_e\Gamma_i}\right)^2 - \left(\frac{1 + \epsilon}{\Gamma_i + \epsilon\Gamma_e}\right)^2\right]^{-1/2} \qquad (10)$$

This velocity is obtained by requiring the Hamiltonians at Q_0^+ and Q_1 to be equal. In summary, for $\bar{k} = 0$ ($VV_{ph} = 1$), there are grey solitons (homoclinic orbits $Q_0^+ - Q_0^+$), dark solitons (heteroclinic orbits $Q_0^+ - Q_0^-$) and shock waves (heteroclinic orbits $Q_0^+ - Q_1$).

III. QUASINEUTRAL PLASMA AND SMALL AMPLITUDE WAVES

We start the analysis of Sys. (4)-(5) by first looking at the long wavelength and small amplitude limit. Under these conditions the quasineutral approximation $\phi'' << n_e - n_i$ is valid and, setting $\phi'' = 0$ in Eq. (5), the potential can be written as a function of the vector potential amplitude (see Ref. [32])

$$\phi = \frac{(\gamma_i - \epsilon\gamma_e)(\Gamma_i\gamma_e - \Gamma_e\gamma_i)}{1 - \epsilon^2} \tag{11}$$

Substituting this relationship in Eq. (4) and keeping terms of third order in a and first order in ϵ, one finds

$$a'' = \left[1 - \bar{\omega}^2 + \epsilon + \frac{\epsilon - V^2}{2V^2}a^2 + \bar{k}^2\frac{a_0^4}{a^4} - \frac{\epsilon a_0^2}{2V^2}\right]a \tag{12}$$

Equation (12) is equivalent to Eq. (40) in Ref. 32 but it also includes the phase modulation effect.

In order to discuss the solitary waves, it is necessary to look at the fixed points of Eq. (12) and their stability. One readily finds that the fixed point $Q_0^\pm$ given by $(a,\ a') = (\pm a_0,\ 0)$ exists only if $\bar{\omega}^2 = \bar{k}^2 + 1 + \epsilon - a_0^2/2$ [the small amplitude limit of Eq. (8)]. Using this condition Eq. (12) becomes

$$a'' = -\frac{\epsilon - V^2}{2V^2}a\left(a_0^2 - a^2\right) + \bar{k}^2\left(\frac{a_0^4}{a^4} - 1\right)a \tag{13}$$

In addition to $Q_0^\pm$, Eq. (13) has two additional fixed points given by $Q_*^\pm = \left(\pm\frac{a_0}{2}\sqrt{\Omega^2 + \Omega\sqrt{\Omega^2+8}}, 0\right)$, that coalesce to $Q_* \equiv (0,\ 0)$ for $\bar{k} = 0$. Here $\Omega \equiv 2V\bar{k}/\left(a_0\sqrt{\epsilon - V^2}\right)$. On the other hand, the stability of $Q_0^\pm$ is given by the eigenvalues $\lambda_{1,2} = \pm\frac{2\bar{k}}{\Omega}\sqrt{1-\Omega^2}$ and, therefore, solitary waves connecting with $Q_0^\pm$ are only possible if $0 < \Omega^2 < 1$, or $V < a_0\sqrt{\epsilon/\left(a_0^2 + 4\bar{k}^2\right)}$ ($Q_0^\pm$ are saddle points). We remark that this condition correspond to very small velocities (the square root of the ratio of the electron to the ion masses ϵ with a correction due to the phase modulation). One also readily verifies that in the regime $\Omega < 1$, Q^* and $Q_*^\pm$ are centers.

The above information about the existence and stability of the fixed points is very helpful to understand the dynamics of the solitary waves. For $\bar{k} = 0$, Eq. (13) admits two dark solitary waves (heteroclinic connection $Q_0^{\mp} - Q_0^{\pm}$) given by [32]

$$a = \pm a_0 \tanh \kappa\xi \tag{14}$$

with the inverse width $\kappa \equiv a_0\sqrt{\epsilon - V^2}/2V$. The two dark solitary waves can be seen in panel (a) of Fig. 1 where we plotted the phase space $a - a'$. The topology of the phase space consists in two heteroclinic orbits connecting the saddle fixed points $Q_0^{\pm}$ and surrounding the fixed point Q^* which is a center. In panel (b) we show the amplitude of the vector potential and the potential versus ξ for the dark solitary wave $Q_0^- - Q_0^+$.

Clearly, the dynamics must be different for $\bar{k} \neq 0$. In first place, Q_* splits in the two fixed points $Q_*^{\pm}$. In second place the dark solitary waves are destroyed because they cannot cross the plane $a = 0$ due to the divergence of the term $\bar{k}^2 a_0^4/a^4$ in Eq. (13). However, even though dark solitary waves (heteroclinic orbits $Q_0^{\pm} - Q_0^{\mp}$) are impossible, one still can find an analytical expression for two grey solitary waves (homoclinic connections $Q_0^{\pm} - Q_0^{\pm}$)

$$a = \pm a_0 \sqrt{\Omega^2 + (1 - \Omega^2) \tanh^2 \left(\sqrt{1 - \Omega^2}\kappa\xi\right)} \tag{15}$$

that becomes Eq. (14) when $\bar{k} = 0$ ($\Omega = 0$). The minimum of the amplitude of these waves is equal to $a_{min} \equiv 2V\bar{k}/\sqrt{\epsilon - V^2}$. The phase space $a - a'$ and a grey solitary wave for $\bar{k} = 0.1$ are plotted in Fig. 1 [panels (c) and (d) respectively]. We see that the trajectories never cross the plane $a = 0$ and both Q_0^+ and Q_0^- have an homoclinic orbit that surrounds the fixed points Q_*^+ and Q_*^- respectively.

Even though the dark and the grey solitary waves are different from the point of view of the dynamical system, physically they both represent a localized depression in the amplitude of the vector potential and a well in the electrostatic potential [see panels (b) and (d) in Fig. 1]. As we will see, the main difference between both waves is related with their phases. A dark wave is a heteroclinic connection $Q_0^+ - Q_0^-$ and it introduces a phase shift equal to π, thus reversing the sign of the magnetic field across the wave. On the other hand, the phase of a grey wave is found by integrating Eq. (6) with the condition $\theta = 0$ as $\xi \to -\infty$

$$\theta = \tan^{-1}\left[\frac{\sqrt{1 - \Omega^2}}{\Omega} \tanh\left(\sqrt{1 - \Omega^2}\kappa\xi\right)\right] + \tan^{-1}\left(\frac{\sqrt{1 - \Omega^2}}{\Omega}\right) \tag{16}$$

Therefore the phase as $\xi \to +\infty$ is $\theta_\infty \equiv 2\tan^{-1}\left(\sqrt{1 - \Omega^2}/\Omega\right)$. We see that when $\Omega \to 0$ ($\bar{k} \to 0$) it becomes $\theta_\infty = \pi$ thus approaching the behaviour of dark waves. On the other

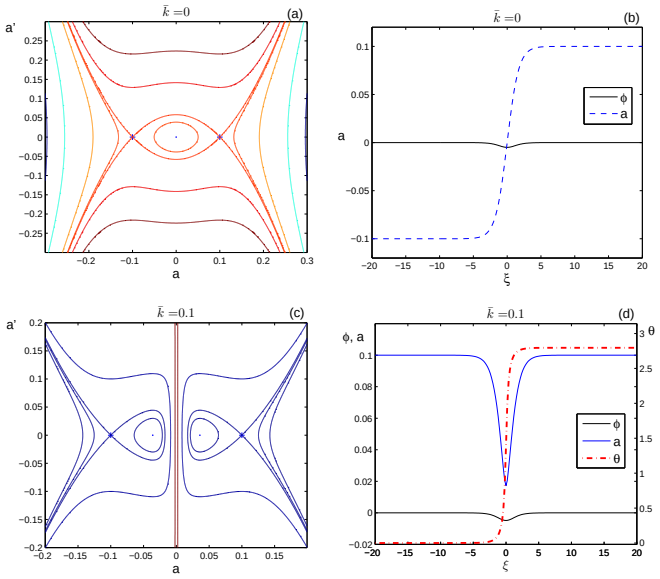

FIG. 1: (Color online) Panels (a) and (b) [(c) and (d)] show the phase space $a - a'$ and the dark (grey) solitary wave respectively at $a_0 = 0.1$ and $V = 0.002$ and $\bar{k} = 0$ ($\bar{k} = 0.1$). The fixed points $Q_0^{\pm}$ are marked with crosses and Q_* (for $\bar{k} = 0$) and $Q_*^{\pm}$ (for $\bar{k} = 0.1$) with a dot.

hand, increasing the value of Ω reduces the phase shift introduced by the solitary wave and it vanishes when $\Omega \to 1$ (we recall that $Q_0^{\pm}$ are saddle points only if $\Omega^2 < 1$).

IV. LARGE AMPLITUDE SOLITARY WAVES

This section deals with the dynamics of the solitary waves with $\bar{k} \neq 0$ and arbitrary amplitudes that are described by Eqs. (4)-(6). Following the procedure of Sec. III, the result will be compared with the case $\bar{k} = 0$ that was investigated in Refs. 3, 29 and 30. As we will see, most of the new features exhibited for the small amplitudes case, like the destruction of the dark solitary waves due to the divergence of the term $\bar{k}^2 a_0^4/a^4$ in Eq. (4), also occur in the general case. However, there are some comments about the organization or existence of the solitary waves in the parametric $V - \bar{\omega} - \bar{k}$ space that must be taken into account.

As already mentioned in Sec. I, the way in which the solitary waves are organized in the parametric space (also known as the spectrum in the literature) can be inferred by geometrical arguments involving the dimensions of the stable and unstable manifolds of the

fixed points and the dimension of the phase space. These geometrical arguments are based on the fact that homoclinic (heteroclinic) orbits lie in the intersection of the stable and the unstable manifolds of the same (different) fixed point(s). We recall that the stable (unstable) manifold of a fixed point Q_i, that we denote by W_i^s (W_i^u), is the set of forward (backward) in ξ trajectories that terminate at Q_i. Note also that the Hamiltonian [Eq. (7)] is conserved and the the intersection of the stable and unstable manifold has to take place within the manifold $H = H_0$, with H_0 the value of the Hamiltonian at $Q_0^{\pm}$.

Let us first apply this geometrical reasoning to the case of small amplitude waves studied in Sec. III. Thanks to the quasineutral approximation we found a relation of the type $\phi = \phi(a)$ [Eq. (11)] and the dimension of the phase space was lowered from four to two. Then, in parametric domains where $Q_0^{\pm}$ are saddle points ($\Omega < 1$), the stable and unstable manifolds of the fixed points $Q_0^{\pm}$ are 1-dimensional. In this situation both manifolds always intersect (they are the same orbit) and the solitary waves exist for any value of the parameters. This statement can be checked with the analytical solution [Eq. (15)] that is valid for any V, $\bar{\omega}$, and $\bar{k}$ provided that $\Omega < 1$.

For arbitrary large amplitude waves, the phase space is 4-dimensional and, taking into account the energy conservation, solitary waves only exist if the stable and the unstable manifolds intersect within a 3-dimensional space. In parametric domains where $Q_0^{\pm}$ is a saddle-center both manifolds are one-dimensional and they are not, in general, expected to intersect. The condition $W_0^s = W_0^u$ constitutes an additional restriction among the parameters and solitary waves would appear within certain surface (or surfaces) in the $V - \bar{\omega} - \bar{k}$ volume. On the other hand, if the fixed point is a saddle-focus the stable and unstable manifolds are 2-dimensional and they are expected to intersect within a 3-dimensional space. For this latter case it is said that the solitary waves have a continuous spectrum.

A. Stability of the fixed points $Q_0^{\pm}$

We start by delimiting in the parametric $V - \bar{\omega} - \bar{k}$ volume the domains of stability of the fixed points $Q_0^{\pm}$. The stability character is determined by the four eigenvalues, say λ_{1-4},

of the Jacobian matrix of Sys. (4)-(5). We find $\lambda^2_{1-4} = -\delta \pm \sqrt{\Delta}$ with

$$\delta \equiv \frac{1-V^2}{2V^2}\left(\frac{1}{\Gamma_e^3}+\frac{\epsilon}{\Gamma_i^3}\right)+2\bar{k}^2>0 \tag{17}$$

$$\Delta \equiv (2\bar{k}^2-\frac{1-V^2}{2V^2}\beta_1)^2-\frac{(1-V^2)}{V^4}\beta_2^2 \tag{18}$$

where $\beta_1 \equiv (\Gamma_e^2+a_0^2)/\Gamma_e^3+\epsilon(\Gamma_i^2+\epsilon^2 a_0^2)\Gamma_i^3$ and $\beta_2 \equiv (1-\epsilon^2)a_0/(\Gamma_e\Gamma_i)^2$. The fixed points $Q_0^{\pm}$ are or saddle-focus type if $\Delta<0$, saddle-centers if $\sqrt{\Delta}>\delta>0$ and centers if $0<\sqrt{\Delta}<\delta$.

The condition $\sqrt{\Delta}=\delta$ yields the velocity values that separate the stability domains where $Q_0^{\pm}$ are saddle-centers and centers

$$V_{SC} \equiv \sqrt{\frac{(\Gamma_i^3+\epsilon^3\Gamma_e^3)(\Gamma_i+\epsilon\Gamma_e)a_0^2-(1-\epsilon^2)^2a_0^2}{(\Gamma_i^3+\epsilon^3\Gamma_e^3)(\Gamma_i+\epsilon\Gamma_e)a_0^2+4\bar{k}^2(\Gamma_i+\epsilon\Gamma_e)\Gamma_e^3\Gamma_i^3}} \tag{19}$$

Similarly the condition $\Delta=0$ gives two different velocities that are the boundaries of the domains where $Q_0^{\pm}$ are saddle-foci and centers

$$V_{SF}^{\pm} \equiv \sqrt{\frac{\beta_1^2+4\bar{k}^2\beta_1-2\beta_2^2 \pm 2\sqrt{\beta_2^4+4\bar{k}^2\beta_2^2(\beta_1+4\bar{k}^2)}}{(\beta_1+4\bar{k}^2)^2}} \tag{20}$$

In the limit $\bar{\omega}\to\bar{\omega}_{min}$ ($a_0\to\infty$) the velocities have the asymptotic behaviour $V_{SC}\sim V_{SF}^{\pm}\to 0$. For $\bar{\omega}\to\bar{\omega}_{max}$ ($a_0\to 0$) one has $V_{SC}\to 0$ and the velocities V_{SF}^{+} and V_{SF}^{-} coalesce at the value $V_{SF}^{\pm}\to\sqrt{(1+\epsilon)/(1+\epsilon+4\bar{k}^2)}$.

Figure 2 shows the stability domains of $Q_0^{\pm}$ in the $V-\bar{\omega}$ plane for $\bar{k}=0.2$. The velocities V_{SC} (dashed line) and $V_{SF}^{\pm}$ (solid lines) split the plane in four different regions where the fixed points $Q_0^{\pm}$ can be saddle-centers, saddle-foci or centers (in two disconnected domains). The maximum and minimum values of $\bar{\omega}$ and an inset with a detail around $V\sim 0.07$ are also shown. This diagram has several differences with respect to the case $\bar{k}=0$ (see Fig. 3): (i) the velocity V_{SF}^{+}, that collapses to 1 for $\bar{k}=0$, introduces a new domain in the $V-\bar{\omega}$ plane where $Q_0^{\pm}$ is a center, (ii) the asymptotic behaviour of V_{SC} and $V_{SF}^{\pm}$ have changed; we recall that at $\bar{k}=0$ one has $V_{SC}\sim V_{SF}\to 1$ as $\bar{\omega}\to 0$ and $V_{SC}\to\epsilon/(1-\epsilon+\epsilon^2)$ and $V_{SF}^{\pm}\to 1$ as $\bar{\omega}\to\sqrt{1+\epsilon}$ and (iii) the velocity V_S [see Eq. (10)] does not appear in Fig. 2 because the fixed point Q_1 does not exist for $\bar{k}\neq 0$.

The domains of stability of the fixed points $Q_0^{\pm}$ for different values of $\bar{k}$ are shown in Fig. 3. For $\bar{k}=0$, there are only three different domains of stability and the velocity V_S splits the saddle-center domain in two different parts. As $\bar{k}$ increases, the domain of existence of $Q_0^{\pm}$ happens at higher $\bar{\omega}$ values (for clarity we chose $\bar{k}$ values for which such domains do not

overlap). The saddle-center and saddle-focus domains (where solitary waves are possible) also become narrower for higher $\bar{k}$.

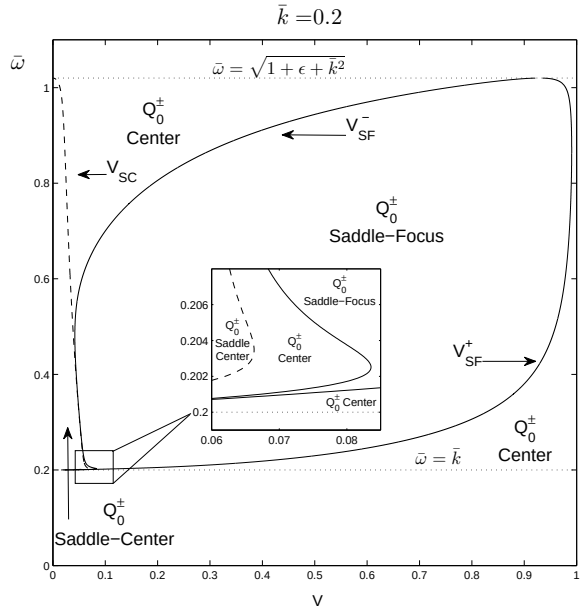

FIG. 2: Characteristic velocity curves and stability domains of the fixed points $Q_0^{\pm}$ in the $V - \bar{\omega}$ plane for $\bar{k} = 0.2$. The inset shows a detail close to $V \sim 0.07$.

B. Solitary waves in the saddle-center domain

When $Q_0^{\pm}$ is a saddle-center, the stable and unstable manifold of $Q_0^{\pm}$ are 1-dimensional and the following shooting method can be used to find the solutions [23]. For fixed $\bar{\omega}$ and $\bar{k}$, Eqs. (4)-(5) are integrated with the initial condition $[\phi \ \dot{\phi} \ a \ \dot{a}] = [0 \ 0 \ a_0 \ 0] + \delta \mathbf{v}_1$ at $\xi = \xi_0$, where $\delta << 1$ and $\mathbf{v}_1$ is the unstable eigenvector of the Jacobian of the system evaluated at $Q_0^{\pm}$. Then, for a homoclinic orbit ($Q_0^{\pm} - Q_0^{\pm}$ connection), both V and ξ_0 are varied until $\phi' = a' = 0$ at $\xi = 0$. In the case of an heteroclinic orbit ($Q_0^{+} - Q_0^{-}$ connection) the conditions are $\phi' = 0$ and $a = 0$ at $\xi = 0$. On the other hand, as can be seen in Fig. 3, the parametric domain where $Q_0^{\pm}$ is a saddle-center represents a small volume of the total parametric space. Therefore, instead of a survey of the branches, we will just look at the transition experienced by some solutions when the parameter $\bar{k}$ changes from zero to a finite value. In order to illustrate this process we have implemented the shooting algorithm with $\delta = 10^{-5}$.

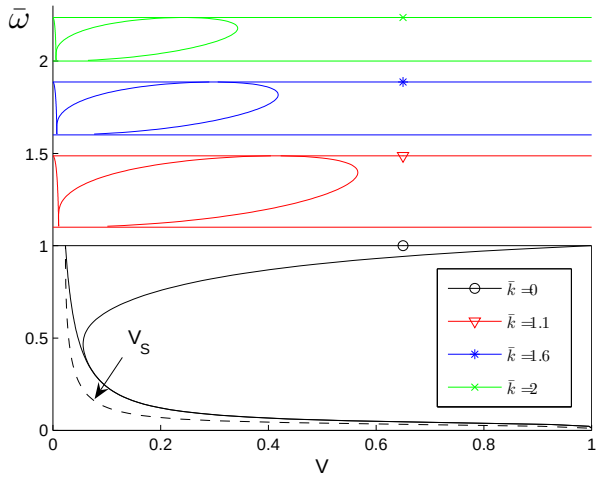

FIG. 3: (Color online) Stability domains of the fixed points $Q_0^{\pm}$ for different $\bar{k}$ values. The velocity V_S of the shock waves at $\bar{k} = 0$ is also shown (dashed line).

For $\bar{k} = 0$, dark and grey solitary waves are possible for velocities values lower and higher than V_S respectively [see i.e. Fig. 3 in Ref. 3]. Examples of these solutions are shown in panels (a) and (c) of Fig. 4. Now, by using the same shooting method and taking a small $\bar{k}$ value (10^{-5}), we find that the grey wave is almost not affected [see panel (d)]. However, the dark wave is destroyed and substituted by a grey wave with a peaky vector potential amplitude at its center for $\bar{k} = 10^{-5}$ [see panel (b)]. This situation is equivalent to the one presented in Sec. III where for $\bar{k} \neq 0$ the dark solitary wave given by Eq. (14) is replaced by the grey wave described by Eq. (15). As already mentioned, whereas the phase space in the low amplitude limit is 2-dimensional and the analytical solution [Eq. (15)] is valid in a continuous range within the $V - \bar{k} - \bar{\omega}$ volume, in the general case the phase space is 4-dimensional and the stable and the unstable manifolds are not expected to intersect. Therefore, the solitary waves appear in surfaces within the $V - \bar{\omega} - \bar{k}$ parametric volume.

C. Solitary waves in the saddle-focus domain

In the saddle-focus domain, the stable and unstable manifolds of $Q_0^{\pm}$ are 2-dimensional and are in general expected to intersect transversally along a 1-dimensional curve that corresponds to the solitary wave. Therefore, for fixed $\bar{k}$, the solitary waves appear in a

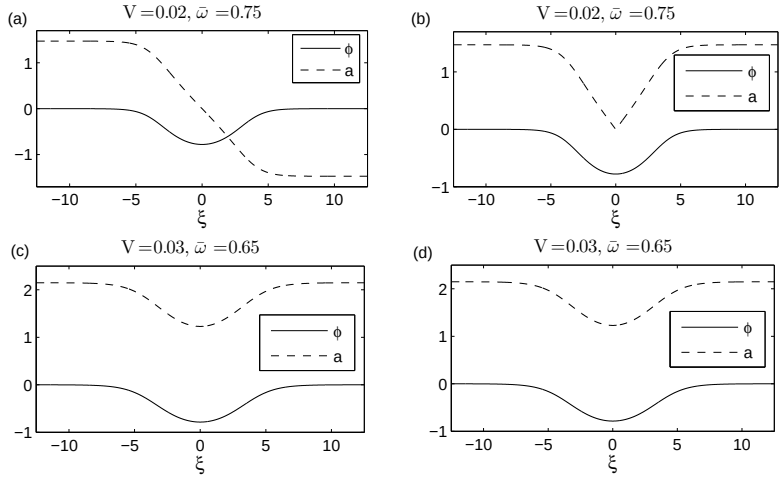

FIG. 4: Solitary waves for $\bar{k} = 0$ [panels (a) and (c)] and $\bar{k} = 10^{-5}$ [panels (b) and (d)]. The dark solitary waves that occur at $\bar{k} = 0$ are destroyed and substituted by grey waves when $\bar{k}$ is finite.

continuous domain within the $V - \bar{\omega}$ plane. They can be computed with the spectral algorithm presented in Ref. 33. The numerical method reduces the set of ordinary differential equations [Eqs. (4) and (5)] to a system of nonlinear algebraic equations that can be solved with a Newton-Raphson method.

Some numerical results are shown in Fig. 5. Shaded regions in panels (a), (b) and (c) display the domain of existence of a certain family of solutions in the $V - \bar{\omega}$ plane for $\bar{k} = 0.2, 0.5$ and 1 respectively. The lines that delimit the domain of existence and stability of $Q_0^{\pm}$ are also represented with dashed lines. We remark that by increasing the parameter $\bar{k}$, it is possible to find solutions in a velocity range where they are not possible (or detected) in previous works for $\bar{k} = 0$. For instance, if $Q_0^{\pm}$ is a saddle-center, the maximum velocity for a solitary wave is $V \sim 0.05$ (see Fig. 3 in Ref. [3]). On the other hand, if $Q_0^{\pm}$ is a saddle-focus, the minimum velocity of a solitary wave is $V \sim 0.32$ (see Fig. 2 in Ref. [30]). Therefore, for $\bar{k} = 0$ there is a gap of velocities where solitary waves do not exist. Now, panels (a), (b) and (c) in Fig. 5 show that this gap can be filled if $\bar{k}$ is increased.

In panel (d) of Fig. 5 the potentials ϕ and a and the phase θ are plotted for a specific solution of this family with parameter values $V = \bar{\omega} = 0.8$ and $\bar{k} = 0.2$. Across the solitary wave there is a jump in the phase θ. From the potentials one can compute the densities [panel (e)] and the electromagnetic fields [panel (f)]. For this value of the frequency the ions are almost not affected by the solitary wave and the electron density exhibits a depression

where an electromagnetic wave is trapped. The charge separation produces an electrostatic field E_x that is balanced by the ponderomotive force of the trapped wave. The solitary wave is embedded in a infinitely long circularly polarized wave because $a \to a_0$ as $\xi \to \infty$. This statement is evident from the B_z component in panel (f).

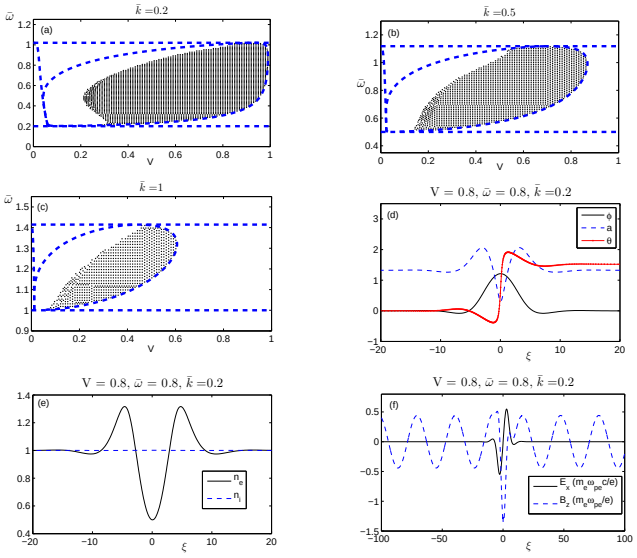

FIG. 5: (Color online) The shaded regions in Panels (a), (b) and (c) display the parametric domain where solitary waves of the type shown in panels (d) exist. The densities and some components of the electromagnetic fields for this specific wave are shown in panels (e) and (f) respectively.

Figure 6 shows some properties of the family of solutions displayed in Fig. 5 as a function of V, $\bar{\omega}$ and $\bar{k}$ [panels (a), (c) and (e) correspond to $\bar{k} = 0.2$ and (b), (d) and (f) to $\bar{k} = 1$]. Top panels (a) and (b) show the maximum kinetic energies of the ions within the solitary wave, $E_i^{max} = max[m_i c^2(\gamma_i - 1)]$. The ions can reach energies of the order of a few MeV, lower than the hundreds of MeV in the case of solitary waves without phase modulation ($\bar{k} = 0$) [30]. This behaviour is due to the enhancement of the minimum allowable value of the frequency ω as the parameter $\bar{k}$ is increased. Note that the ion response, and therefore their energies, is weaker for higher values of the frequency

The breaking of the solitary waves with VBC has been also proposed as an additional mechanism for the generation of fast ions [2, 32]. In this case, the solitary waves are organized in branches in the $V - \bar{\omega}$ plane which end at the breaking velocity V_{br} ($V_{br} \sim 0.32$ for single-hump waves) where the density profile exhibits a cusp profile. The authors estimated the

energy gained by the ions during the wavebreaking by $E_{ion} \sim \phi_{br}/(1-V_{br})$ [2, 32]. Similarly, in Ref. 30 it was shown that the boundary of existence for the solution in panels (a), (b) and (c) of Fig. 5 is due to a bifurcation mechanism known as coalescence [31, 34, 35]. In the case of wavebreaking, we can follow the reasoning of Refs. 2 and 32 and estimate the energy gained by the ions by using the maximum value of the potential given in panels (c) and (d) of Fig. 6. For instance, for $\bar{k} = 0.2$, the maximum potential $\phi_{max} \sim 50$ is reached for $V \sim 0.3$ that gives an energy $E_i \sim 35MeV$.

On the other hand, panels (e) and (f) in Fig. 6 show the phase shift θ_∞ in the range $-\pi < \theta_\infty < \pi$ introduced by the solitary waves. We observe that for $\bar{k} = 0.2$ it varies from 0 at $\bar{\omega} \sim \bar{\omega}_{min}$ to π at $\bar{\omega} \sim \bar{\omega}_{max}$. In the case $\bar{k} = 1$, the phase shift is small and uniform in the $V - \bar{\omega}$ plane.

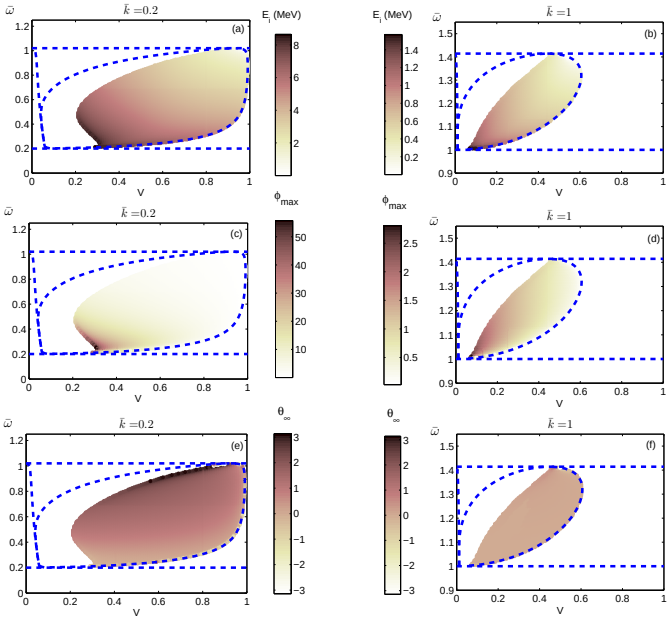

FIG. 6: (Color online) Some properties of the family of solitary waves shown in Fig. 5. Panels (a), (c) and (e) show the maximum values of the ion energy E_i, the maximum values of the potential ϕ_{max} and the phase shift θ_∞ for $\bar{k} = 0.2$, respectively. Panels (b), (d) and (f) display the same quantities for $\bar{k} = 1$.

The system admits other types of families of solitary waves, even though the domains of existence could vary from one family to another. Other examples of solitary waves are shown in Fig 7. Unlike the family in Fig. 5, which has a potential ϕ with a hump in the center of

the wave, the solitary wave in panel (a) of Fig. 7 has a depression in ϕ. Similarly to the dark solitary wave with VBC [32], this effective well formed by the radiation pressure can trap positively charged ions and accelerate them. Another interesting feature is the existence of solitary waves with several humps. It is well-known from the theory of dynamical system that, if for certain given parameters the fixed point is a saddle-focus and a homoclinic orbit exists, then there exist infinitely many multi-hump homoclinic orbits [36]. Panel (b) in Fig. 7 shows an example of a two-hump solitary wave at exactly the same parameter value as the wave shown in Fig. 5. Clearly, each hump introduced a jump in the phase θ.

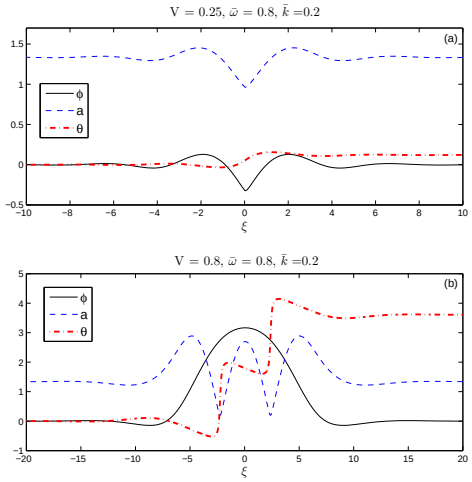

FIG. 7: (Color online) Some examples of solitary waves in the domain where the fixed points $Q_0^{\pm}$ are saddle-foci.

V. CONCLUSIONS

In the last two decades particle-in-cell simulations [1, 2, 4–9] and laboratory experiments [9–15] have shown the excitation of relativistic solitary waves during the interaction of a high-intensity laser pulse with an underdense plasma. They produce different interesting phenomena like the emission of electromagnetic bursts when they reach the plasma-vacuum interface [5] or holes in the plasma density (also called post-solitons) where ions are accelerated [37]. The breaking of solitary waves can also provide an additional mechanism for the generation of fast ions in laser irradiated plasmas [27]. In this work we have discussed the existence of phase modulated solitary waves embedded in an infinitely long circularly

polarized electromagnetic wave in plasmas. These waves are exact nonlinear solutions with nonvanishing boundary conditions (NVBC) of the Maxwell-fluid equations for a cold plasma composed of electrons and ions.

The main properties of the waves as a function of their group velocities, wavevectors and frequencies have been investigated with special attention to the limit of small amplitude waves. We emphasized the role of the fixed point where the solitary waves connect, since its stability determines how the waves are organized depending on the above cited parameters. In particular, we have have derived analytically the critical velocities that dictate the parametric domains where the solitary waves do not exist, exist in branches, or form a continuum. In a second step, the implementation of a spectral algorithm allowed to compute different families of solutions and their domains of existence.

As compared to previous works [3, 29, 30], the solitary waves with phase modulation present two important new aspects. First, by changing the parameter $\bar{k}$ that controls the nonlinear phase modulation, it is possible to modify the phase shift introduced in the infinitely long electromagnetic wave. For instance, we have shown in the small amplitude limit that the dark wave ($\bar{k} = 0$) has a phase shift equal to π and it reverses the sign of the magnetic field. However, by including the phase modulation ($\bar{k} \neq 0$), a grey wave with the desirable phase shift and the same physical properties, i.e. the same type of ϕ profile, can be obtained. The second difference involves the parametric regime where solutions exist. Whereas non-modulated solitary waves are not possible (or at least were not detected [3, 29, 30]) within the group velocity range $0.05c - 0.32c$, the addition of a phase modulation allows the construction of solutions in this range.

The experimental excitation of solitary waves with NVBC is still an open problem. It is well known that solitary waves with vanishing boundary conditions (VBC) are spontaneously excited during laser-plasma interaction [1] but, to the best of our knowledge, they have never been observed embedded in long laser pulses. A long laser pulse with a localized amplitude modulation could probably excite solitary waves with NVBC. A similar scheme but with a short pulse was proposed to excite solitary wave with VBC [24].

The solitary waves studied here can also be interpreted as the stationary state after the collision of a long laser pulse and a solitary wave with VBC [30]. We now propose that solitary waves with NVBC could be excited by using two laser pulses. First, a short laser pulse with frequency above (but close to) the electron plasma frequency ω_{pe} would excite

solitary waves with VBC. In second place, if a second long pulse is able to interact with one of the solitary waves, it could become embedded in the long pulse. Previous works [3, 29, 30] would predict a phase shift across the long laser pulse equal to 0 or π depending on the type of solitary wave (grey or dark). However, the phase shift of the more general solutions studied in the present work could take intermediate values that would depend on the particular conditions of the interaction. According to the theoretical predictions, it would be controlled by the type of solitary wave, its group velocity and the amplitude and frequency of the laser. We finally remark that a similar scheme with two laser pulses has been proposed to generate ultrashort electromagnetic pulses [38]. Unlike our case, the second laser pulse must be short and it produces the ultrashort wave during the interaction with the solitary wave.

Acknowledgments

G. Sanchez-Arriaga is supported by ANR under the GOSPEL project, grant reference ANR-08-BLAN-0072-03. This work was performed using HPC resources at CCRT and CINES made available by GENCI under grants 2010056304 and 2011056304.

APPENDIX A: THE LIMIT CASE $V = 0$ AND $v_{ex} = 0$ WITH IMMOBILE IONS

Here we study a plasma with fixed ions in the double limit of vanishing group velocity for the solitary wave ($V \to 0$) and vanishing longitudinal electron velocity ($v_{ex} \to 0$). In this situation, taking $\mathbf{P}_e = 0$, one has $\gamma_e = \sqrt{1+a^2}$ and the longitudinal component of Eq. (2d) gives $\phi = \sqrt{1+a^2} - \Gamma_e$. Equation (2a) yields $n_e = 1 + \phi''$ and, substituting in Eq. (4), a single equation for the amplitude of the vector potential is obtained

$$\frac{a''}{1+a^2} + \left[\bar{\omega}^2 - \bar{k}^2 \frac{a_0^4}{a^4} - \frac{1}{\sqrt{1+a^2}} - \frac{a'^2}{(1+a^2)^2}\right] a = 0 \tag{A1}$$

For solutions with VBC ($a \to 0$ as $\xi \to 0$) we recall that the condition $\bar{k} = 0$ holds whereas for NVBC ($a \to 0$ as $\xi \to -\infty$) one has the dispersion relationship $\bar{\omega}^2 = \bar{k}^2 + \Gamma_e^{-1}$.

The existence of solitary waves can be discussed by looking at the stability properties of the fixed point where the homoclinic orbits connects. For instance, for VBC, the fixed point $(a,\ a') = (0,\ 0)$ of Eq. (A1) has eigenvalues $\lambda_{1,2} = \pm\sqrt{1-\bar{\omega}^2}$ and it is a saddle. The

solitary wave has an analytical form given by [26]

$$a = \frac{2\sqrt{1-\bar{\omega}^2}\cosh\left(\sqrt{1-\bar{\omega}^2}\xi\right)}{\cosh^2\left(\sqrt{1-\bar{\omega}^2}\xi\right)+\bar{\omega}^2-1} \tag{A2}$$

In this case the phase space is 2-dimensional and the (1-dimensional) stable and unstable manifolds of the fixed point always intersect. This geometrical argument justifies the appearance of solutions in a continuous range of $\bar{\omega}$. However, for NVBC the eigenvalues of the fixed point $(a,\ a') = (a_0,\ 0)$ are $\lambda_{1,2} = \pm i\sqrt{4\Gamma_e\bar{k}^2 + a_0^2/\Gamma_e}$. Hence, for immobile ions, $V = 0$, $v_{ex} = 0$ and NVBC, the fixed point is a center and solitary waves do not exist.

[1] S. V. Bulanov, T. Z. Esirkepov, N. M. Naumova, F. Pegoraro, and V. A. Vshivkov, Phys. Rev. Lett. **82**, 3440 (1999).

[2] S. V. Bulanov, F. Califano, T. Z. Esirkepov, K. Mima, N. M. Naumova, K. Nishihara, F. Pegoraro, Y. Sentoku, and V. A. Vshivkov, Physica D **152**, 682 (2001).

[3] D. Farina and S. V. Bulanov, Plasma Phys. Controlled Fusion **47**, A260000 (2005).

[4] S. V. Bulanov, I. N. Inovenkov, V. I. Kirsanov, N. M. Naumova, and A. S. Sakharov, Phys. Fluids B **4**, 1935 (1992).

[5] Y. Sentoku, T. Z. Esirkepov, K. Mima, K. Nishihara, F. Califano, F. Pegoraro, H. Sakagami, Y. Kitagawa, N. M. Naumova, and S. V. Bulanov, Phys. Rev. Lett. **83**, 3434 (1999).

[6] N. M. Naumova, J. Koga, K. Nakajima, T. Tajima, T. Z. Esirkepov, S. V. Bulanov, and F. Pegoraro, Phys. Plasmas **8**, 4149 (2001).

[7] T. Esirkepov, K. Nishihara, S. V. Bulanov, and F. Pegoraro, Phys. Rev. Lett. **89**, A265002 (2002).

[8] T. Esirkepov, S. V. Bulanov, K. Nishihara, and T. Tajima, Phys. Rev. Lett. **92**, 255001 (2004).

[9] G. Sarri, D. K. Singh, J. R. Davies, F. Fiuza, K. L. Lancaster, E. L. Clark, S. Hassan, J. Jiang, N. Kageiwa, N. Lopes, et al., Phys. Rev. Lett. **105**, 175007 (2010).

[10] M. Borghesi, S. Bulanov, D. H. Campbell, R. J. Clarke, T. Z. Esirkepov, M. Galimberti, L. A. Gizzi, A. J. MacKinnon, N. M. Naumova, F. Pegoraro, et al., Phys. Rev. Lett. **88**, 135002 (2002).

[11] M. Borghesi, D. H. Campbell, A. Schiavi, M. G. Haines, O. Willi, A. J. MacKinnon, P. Patel, L. A. Gizzi, M. Galimberti, R. J. Clarke, et al., Phys. Plasmas **9**, 2214 (2002).

[12] L. M. Chen, H. Kotaki, K. Nakajima, J. Koga, S. V. Bulanov, T. Tajima, Y. Q. Gu, H. S. Peng, X. X. Wang, T. S. Wen, et al., Phys. Plasmas **14**, 040703 (2007).

[13] A. S. Pirozhkov, J. Ma, M. Kando, T. Z. Esirkepov, Y. Fukuda, L. Chen, I. Daito, K. Ogura, T. Homma, Y. Hayashi, et al., Phys. Plasmas **14**, 123106 (2007).

[14] M. Kando, A. S. Pirozhkov, Y. Fukuda, T. Z. Esirkepov, I. Daito, K. Kawase, J. L. Ma, L. M. Chen, Y. Hayashi, M. Mori, et al., European Physical Journal D **55**, 465 (2009).

[15] L. Romagnani, A. Bigongiari, S. Kar, S. V. Bulanov, C. A. Cecchetti, T. Z. Esirkepov, M. Galimberti, R. Jung, T. V. Liseykina, A. Macchi, et al., Phys. Rev. Lett. **105**, 175002 (2010).

[16] S. Poornakala, A. Das, P. K. Kaw, A. Sen, Z. M. Sheng, Y. Sentoku, K. Mima, and K. Nishikawa, Phys. Plasmas **9**, 3802 (2002).

[17] M. Lontano, M. Passoni, and S. V. Bulanov, Phys. Plasmas **10**, 639 (2003).

[18] D. Farina, M. Lontano, and S. Bulanov, Phys. Rev. E **62**, 4146 (2000).

[19] J. Borhanian, I. Kourakis, and S. Sobhanian, Phys. Lett. A **373**, 3667 (2009).

[20] J. H. Marburger and R. F. Tooper, Physical Review Letters **35**, 1001 (1975).

[21] C. S. Lai, Physical Review Letters **36**, 966 (1976).

[22] N. L. Tsintsadze and D. D. Tskhakaia, Zhurnal Eksperimental noi i Teoreticheskoi Fiziki **72**, 480 (1977).

[23] V. A. Kozlov, A. G. Litvak, and E. V. Suvorov, JETP **49**, 75 (1979).

[24] P. K. Kaw, A. Sen, and T. Katsouleas, Phys. Rev. Lett. **68**, 3172 (1992).

[25] H. H. Kuehl and C. Y. Zhang, Phys. Rev. E **48**, 1316 (1993).

[26] T. Z. Esirkepov, F. F. Kamenets, S. V. Bulanov, and N. M. Naumova, JETP Lett **68**, 36 (1998).

[27] D. Farina and S. V. Bulanov, Phys. Rev. Lett. **86**, 5289 (2001).

[28] S. Poornakala, A. Das, A. Sen, and P. K. Kaw, Phys. Plasmas **9**, 1820 (2002).

[29] D. Farina and S. V. Bulanov, in *Superstrong Fields in Plasmas*, edited by M. Lontano, G. Mourou, O. Svelto, & T. Tajima (2002), vol. 611 of *American Institute of Physics Conference Series*, pp. 151–156.

[30] G. Sánchez-Arriaga, E. Siminos, and E. Lefebvre, Plasma Phys. and Control. Fusion **53**, 045011 (2011).

[31] A. R. Champneys, Physica D **112**, 158 (1998).

[32] D. Farina and S. V. Bulanov, Plasma Phys. Rep. **27**, 641 (2001).

[33] Y. Liu, L. Liu, and T. Tang, J. Comput. Phys. **111**, 373 (1994).

[34] B. Buffoni, A. R. Champneys, and J. F. Toland, J. Dyn. Diff. Eq. **8**, 221 (1996).

[35] J. Knobloch, J. Dyn. Differ. Equ. **9**, 427 (1997).

[36] R. Devaney, J. Differential Equations **26**, 247 (1976).

[37] N. M. Naumova, S. V. Bulanov, T. Z. Esirkepov, D. Farina, K. Nishihara, F. Pegoraro, H. Ruhl, and A. S. Sakharov, Phys. Rev. Lett. **87**, 185004 (2001).

[38] S. S. Bulanov, T. Z. Esirkepov, F. F. Kamenets, and F. Pegoraro, Phys. Rev. E **73**, 036408 (2006), arXiv:physics/0511196.